Attitude observer on the special orthogonal group with earth velocity estimation

Daniel Viegas, Pedro Batista, Paulo Oliveira, and Carlos Silvestre

Systems & Control Letters, vol. 126, pp. 33-39, April 2019

https://doi.org/10.1016/j.sysconle.2019.03.001

Attitude Observer on the Special Orthogonal Group with Earth Velocity Estimation

Pedro Batista[a], Carlos Silvestre[b], Paulo Oliveira[c]

[a] *Institute for Systems and Robotics, LARSyS, Instituto Superior Técnico, Universidade de Lisboa, Portugal. Corresponding author.*
[b] *Department of Electrical and Computer Engineering, Faculty of Science and Technology, University of Macau, Macau, on leave from the Instituto Superior Técnico, Universidade de Lisboa, Portugal*
[c] *Institute for Systems and Robotics, LARSyS, Department of Mechanical Engineering, Instituto Superior Técnico, Universidade de Lisboa, Portugal*

Abstract

This paper proposes a new nonlinear attitude observer based on high-grade rate gyros and single body-fixed vector measurements of a constant inertial vector, in contrast with typical solutions that require two of these vectors. The structure is cascaded, where in the first block a vector that is related to the angular velocity of the Earth is estimated and in the second block the attitude itself is obtained. The attitude is directly estimated on the special orthogonal group and the estimation error is shown to converge to zero, with a region of convergence that is best described as semi-global, with local exponential convergence. Simulation results illustrate the achievable performance of the proposed solution and the robustness to sensor noise.

Key words: Attitude algorithms; state observers; navigation systems; estimation algorithms; nonlinear systems.

1. Introduction

Attitude estimation has long attracted the interest of the scientific community. On one hand, it is of paramount importance for the operation of autonomous vehicles. On the other hand, it is a very interesting and challenging topic of research. Algebraic solutions (see [1]) based on vector observations of known inertial vectors do not effectively fuse all the information that is typically available, e.g. angular velocity measurements provided by rate gyros, and therefore do not exhibit any filtering effects. In the survey [2] many different filtering solutions have been reviewed. As in most nonlinear estimation problems, the extended Kalman filter (EKF) was the workhorse of earlier solutions. However, the divergence due to the linearization errors of the EKF [2] has paved the way for the pursuit of alternative designs with convergence guarantees, in particular nonlinear observers, see e.g. [3], [4], [5], [6], [7], [8], [9], and references therein. Another interesting topic of research on attitude estimation is that of optimal filtering, see e.g. [10]. In [11] a deterministic attitude estimator is presented based on uncertainty ellipsoids. Previous work by the authors can be found in [12] and [13].

The majority of the attitude solutions assume that there exist, at least, two body-fixed measurements of corresponding known constant vectors in inertial coordinates, with a few exceptions in [14], [15], [16], [17], and [18], where time-varying reference vectors are considered and some form of persistency-of-excitation is required. The main contribution of this paper is a novel attitude observer based on: i) measurements of a single body-fixed vector, whose inertial counterpart is known and constant; and ii) high-grade rate gyro measurements that are sensitive to the angular rotation of the Earth. In contrast with the aforementioned references, the single body-fixed vector that is measured corresponds to a constant inertial vector. This could be of potential interest in long underwater missions in scenarios with strong magnetic anomalies, which would invalidate the use of the magnetic field, one of two quantities that are usually employed in attitude estimation. Notice that, overall, the idea of the paper is closer to the first, and more popular, class of solutions that demand the existence of at least two body-fixed measurements of corresponding known constant vectors in inertial coordinates. However, only one body-fixed measurement is assumed available in this paper and a second one is dynamically estimated. Notice also that the designs presented in [17], [15], or [18] cannot be applied in the present case as the only vector observation that is directly available corresponds to a constant vector in inertial coordinates, which does not provide sufficient information for attitude estimation.

The observer that is proposed in the paper has a cascade structure [19]. In the first block an estimate of a second body-fixed vector is obtained, related to the Earth angular velocity, whose counterpart in inertial coordinates is well known. Then, a second observer fuses the measurements of the high-grade rate gyros and the two vectors available to obtain a filtered version of the attitude of the platform. The error of the estimate of the second vector required for attitude estimation, provided by the first observer, is shown to converge to zero for all initial conditions. The attitude error of the second observer, considering the cascade structure, is shown to converge to zero, with a large basin of attraction. The overall error dynamics are also shown to be locally exponentially stable. A solution to the problem addressed here was first presented in the preliminary work [20]. This paper offers a comprehensive study and

Email addresses: pbatista@isr.tecnico.ulisboa.pt (Pedro Batista), csilvestre@umac.mo (Carlos Silvestre), pjcro@isr.tecnico.ulisboa.pt (Paulo Oliveira)

proofs of modified versions of the observers, including additional results, and a thorough performance evaluation resorting to Monte Carlo runs. The observers that are now proposed also offer a significant advantage as they avoid a potential problem present in [20], as it will be discussed later on.

An alternative solution to the problem addressed in this paper was proposed in [21], where global stability results are achieved at the expense of the topological characteristics of the estimates, which are ignored in the design but verified asymptotically. In the present paper, the topological characteristics of the quantities are preserved by construction, following the more popular paradigm in attitude estimation, and hence global stability results cannot be achieved through continuous feedback.

Throughout the paper the symbol $\mathbf{0}$ denotes a matrix of zeros and $\mathbf{I}$ an identity matrix, both of appropriate dimensions. For $\mathbf{x} \in \mathbb{R}^3$ and $\mathbf{y} \in \mathbb{R}^3$, $\mathbf{x} \cdot \mathbf{y}$ and $\mathbf{x} \times \mathbf{y}$ represent the inner and cross products, respectively. For convenience, define also the transpose operator $(.)^T$, and notice that $\mathbf{x} \cdot \mathbf{y} = \mathbf{x}^T\mathbf{y}$, $\mathbf{x}, \mathbf{y} \in \mathbb{R}^3$. The special orthogonal group is denoted by $SO(3) := \left\{\mathbf{X} \in \mathbb{R}^{3\times3} : \mathbf{X}\mathbf{X}^T = \mathbf{X}^T\mathbf{X} = \mathbf{I} \wedge \det(\mathbf{X}) = 1\right\}$. The cross product operator is used extensively in the paper, as well as operations involving elements of $SO(3)$. In compact matrix form, $\mathbf{S}(\mathbf{x}) \in \mathbb{R}^{3\times3}$ is the skew-symmetric matrix that encodes the cross product, i.e., $\mathbf{S}(\mathbf{x})\,\mathbf{y} = \mathbf{x} \times \mathbf{y} \quad \mathbf{x}, \mathbf{y} \in \mathbb{R}^3$.

2. Problem statement

Consider a robotic platform where a set of three, high-grade, orthogonally mounted rate gyros are available, in addition to another sensor, possibly inertial, that measures, in the reference frame of the platform, a vector that is constant in some inertial frame. Further consider that the rate gyros are good enough to be sensitive to the angular velocity of the Earth about its own axis. Loosely speaking, the problem addressed in the paper is that of determining the attitude of the platform.

To set the problem framework, let $\{I\}$ denote a local inertial coordinate reference frame, e.g. the North-East-Down (NED) coordinate frame with the origin fixed to some point of the Earth, and denote by $\{B\}$ the so-called body-fixed frame, attached to the platform. It is assumed, without loss of generality, that this is also the frame of the sensors. Notice that due to the rotation and curvature of the Earth, the NED coordinate frame is not truly inertial but for local navigation purposes it can be considered so. Let $\mathbf{R}(t) \in SO(3)$ denote the rotation matrix from $\{B\}$ to $\{I\}$, which satisfies

$$\dot{\mathbf{R}}(t) = \mathbf{R}(t)\mathbf{S}\left[\omega(t)\right], \tag{1}$$

where $\omega(t) \in \mathbb{R}^3$ is the angular velocity of $\{B\}$ with respect to $\{I\}$, expressed in $\{B\}$.

The measurements of the high-grade set of rate gyros are given by

$$\omega_m(t) = \omega(t) + \omega_E(t), \tag{2}$$

where $\omega_E(t) \in \mathbb{R}^3$ is the angular velocity of the Earth about its own axis, expressed in $\{B\}$. Denote by ${}^I\omega_E \in \mathbb{R}^3$ the angular velocity of the Earth about its own axis expressed in $\{I\}$. Then, ${}^I\omega_E = \mathbf{R}(t)\omega_E(t)$. Let $\mathbf{m}(t) \in \mathbb{R}^3$ denote the measurements of the second sensor, which measures, in body-fixed coordinates, a vector that, when expressed in inertial coordinates, is assumed to be known and constant. Let ${}^I\mathbf{m} \in \mathbb{R}^3$ denote the inertial vector corresponding to $\mathbf{m}(t)$. Then, similarly to the angular velocity of the Earth about its own axis, one has

$${}^I\mathbf{m} = \mathbf{R}(t)\mathbf{m}(t). \tag{3}$$

The following assumptions are considered throughout the paper.

Assumption 1. *The inertial vector ${}^I\mathbf{m}$ is not parallel to the angular velocity of the Earth ${}^I\omega_E$, i.e., there exists a constant $c_v > 0$ such that $\left\|{}^I\omega_E \times {}^I\mathbf{m}\right\|^2 \geq c_v$.*

Assumption 2. *The signal $\omega_m(t)$ and its derivative $\dot{\omega}_m(t)$ are bounded for all time.*

The first assumption is standard as most attitude estimation solutions assume that there exist, at least two known non-parallel inertial vectors, which are measured in body-fixed coordinates. Yet, in this paper, one of the two vectors, $\omega_E(t)$, is not even measured. Instead, it is also explicitly estimated. The second is a standard technical assumption in attitude estimation, see e.g. [5], [8], [15], and [22], that is evidently verified for all systems in practice, as one cannot have arbitrarily large angular velocities or accelerations.

The problem addressed in the paper is that of designing an observer, with convergence guarantees, for the rotation matrix $\mathbf{R}(t)$ based on the measurements $\omega_m(t)$ and $\mathbf{m}(t)$, as well as the knowledge of both ${}^I\omega_E$ and ${}^I\mathbf{m}$.

3. Observer design

As briefly discussed in the introduction, the idea of the observer that is proposed in the paper is to first obtain an estimate of a second vector $\mathbf{v}(t)$, in body-fixed coordinates, whose counterpart, in inertial coordinates, is constant and known, so that two vectors are available for attitude estimation purposes. Additionally, the angular velocity of the Earth is also required for filtering purposes. This is detailed in Section 3.1, where an auxiliary observer is proposed that preserves the norm of the estimate of the available vector measurement. The attitude observer, which uses, in addition to the sensor measurements, the estimates provided by the auxiliary observer, is proposed in Section 3.2 and its stability is analyzed considering the overall cascade structure. A block diagram of the proposed cascade observer is depicted in Fig. 1, where the outputs of both observers are estimates of the quantities under the hat symbols.

3.1. Auxiliary observer

The time derivative of $\mathbf{m}(t)$ can be written as

$$\dot{\mathbf{m}}(t) = -\mathbf{S}\left[\omega_m(t) - \omega_E(t)\right]\mathbf{m}(t). \tag{4}$$

Suppose, for a moment, that $\mathbf{m}(t)$ is constant and that one only had knowledge of $\mathbf{m}(t)$ and $\omega_m(t)$. Then, it follows from (4) that

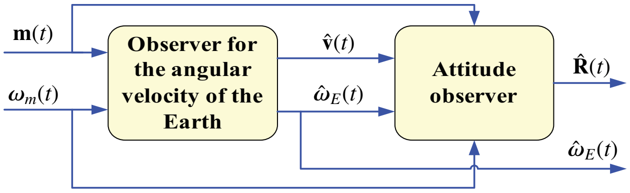

Figure 1: Structure of the cascade attitude observer

it would be impossible to estimate $\boldsymbol{\omega}_E(t)$. However, one should be able to estimate the component of $\boldsymbol{\omega}_E(t)$ that is not parallel to $\mathbf{m}(t)$. Moreover, notice that the component of $\boldsymbol{\omega}_E(t)$ that is parallel to $\mathbf{m}(t)$ does not affect the dynamics of the latter. In light of this, and under Assumption 1, consider the orthogonal decomposition

$$\boldsymbol{\omega}_E(t) = c_1\mathbf{m}(t) - c_2\mathbf{v}(t), \tag{5}$$

with $c_1 := \frac{{}^I\boldsymbol{\omega}_E \cdot {}^I\mathbf{m}}{\|{}^I\mathbf{m}\|^2}$ and $c_2 := \frac{1}{\|{}^I\mathbf{m}\|^2}$, and where $\mathbf{v}(t) := \mathbf{m}(t) \times [\mathbf{m}(t) \times \boldsymbol{\omega}_E(t)]$ is an auxiliary vector. Notice that $\mathbf{v}(t)$ is a body-fixed vector that corresponds to a known constant vector in inertial coordinates, as given by

$$\mathbf{v}(t) = \mathbf{R}^T(t)\,{}^I\mathbf{v}, \tag{6}$$

where ${}^I\mathbf{v} := {}^I\mathbf{m} \times \left({}^I\mathbf{m} \times {}^I\boldsymbol{\omega}_E\right)$ is non-null under Assumption 1. The time derivative of (6) can be written as

$$\dot{\mathbf{v}}(t) = -\mathbf{S}\left[\boldsymbol{\omega}_m(t) - \boldsymbol{\omega}_E(t)\right]\mathbf{v}(t). \tag{7}$$

This is an undesirable expression as the angular velocity of the Earth is not estimated directly. Instead, consider the decomposition (5) in (7) and (4), which allows to write the nominal system dynamics

$$\begin{cases} \dot{\mathbf{m}}(t) = -\mathbf{S}\left[\boldsymbol{\omega}_m(t) + c_2\mathbf{v}(t)\right]\mathbf{m}(t) \\ \dot{\mathbf{v}}(t) = -\mathbf{S}\left[\boldsymbol{\omega}_m(t) - c_1\mathbf{m}(t)\right]\mathbf{v}(t) \end{cases}. \tag{8}$$

Consider the observer for (8) given by

$$\begin{cases} \dot{\hat{\mathbf{m}}}(t) = & -\mathbf{S}\left[\boldsymbol{\omega}_m(t) + c_2\hat{\mathbf{v}}(t) + \alpha_1\mathbf{m}(t)\times\hat{\mathbf{m}}(t)\right]\hat{\mathbf{m}}(t) \\ \dot{\hat{\mathbf{v}}}(t) = & -\mathbf{S}\left[\boldsymbol{\omega}_m(t) - c_1\mathbf{m}(t)\right]\hat{\mathbf{v}}(t) + \alpha_2\mathbf{m}(t)\times\hat{\mathbf{m}}(t) \\ & -\alpha_0\mathbf{m}(t)\cdot\hat{\mathbf{v}}(t)\mathbf{m}(t) \end{cases}, \tag{9}$$

where $\hat{\mathbf{m}}(t) \in \mathbb{R}^3$ and $\hat{\mathbf{v}}(t) \in \mathbb{R}^3$ correspond to the estimates of $\mathbf{m}(t)$ and $\mathbf{v}(t)$, respectively, and $\alpha_0 \in \mathbb{R}^+$, $\alpha_1 \in \mathbb{R}^+$, and $\alpha_2 \in \mathbb{R}^+$ are positive observer gains. Notice that the observer structure is similar to that of the nominal system, with three feedback terms: i) two are additive, to drive $\hat{\mathbf{v}}(t)$, while the other is embedded in such a way that the norm of $\hat{\mathbf{m}}(t)$ is preserved. More insight to the specific structure of the feedback terms will be given later on. Let $\tilde{\mathbf{m}}(t) := \mathbf{m}(t) - \hat{\mathbf{m}}(t)$ and $\tilde{\mathbf{v}}(t) := \mathbf{v}(t) - \hat{\mathbf{v}}(t)$ denote the estimation errors. Then, from (8) and (9), and using the fact that the cross product of vectors is null again, as well as the fact that $\mathbf{v}(t)$ is orthogonal to $\mathbf{m}(t)$, allows to write the error dynamics

$$\begin{cases} \dot{\tilde{\mathbf{m}}}(t) = & -\mathbf{S}\left[\boldsymbol{\omega}_m(t) + c_2\mathbf{v}(t) - c_2\tilde{\mathbf{v}}(t)\right]\tilde{\mathbf{m}}(t) \\ & +\mathbf{S}\left[\alpha_1\mathbf{m}(t)\times\tilde{\mathbf{m}}(t)\right]\tilde{\mathbf{m}}(t) \\ & +\alpha_1\left[\mathbf{m}(t)\times\hat{\mathbf{m}}(t)\right]\times\mathbf{m}(t) \\ & -c_2\tilde{\mathbf{v}}(t)\times\mathbf{m}(t) \\ \dot{\tilde{\mathbf{v}}}(t) = & -\mathbf{S}\left[\boldsymbol{\omega}_m(t) - c_1\mathbf{m}(t)\right]\tilde{\mathbf{v}}(t) + \alpha_2\mathbf{m}(t)\times\tilde{\mathbf{m}}(t) \\ & -\alpha_0\mathbf{m}(t)\cdot\tilde{\mathbf{v}}(t)\mathbf{m}(t) \end{cases}. \tag{10}$$

The following theorem addresses the stability and convergence properties of (10).

Theorem 1. *Consider the state observer* (9)*, with positive observer gains* α_0*,* α_1*, and* α_2*. Further assume that Assumptions 1 and 2 hold. Then, for all initial conditions such that* $\|\hat{\mathbf{m}}(t_0)\| = \left\|{}^I\mathbf{m}\right\|$*, it is true that:*

i) the error variables $\tilde{\mathbf{m}}(t)$ *and* $\tilde{\mathbf{v}}(t)$ *are bounded;*

ii) $\lim_{t\to\infty}\mathbf{m}(t)\times\hat{\mathbf{m}}(t) = \mathbf{0}$; *and*

iii) $\lim_{t\to\infty}\tilde{\mathbf{v}}(t) = \mathbf{0}$.

Proof. Consider the Lyapunov candidate function

$$V\left(\tilde{\mathbf{m}}(t), \tilde{\mathbf{v}}(t)\right) := \frac{1}{2}\|\tilde{\mathbf{m}}(t)\|^2 + \frac{1}{2}\frac{c_2}{\alpha_2}\|\tilde{\mathbf{v}}(t)\|^2,$$

which is positive definite as both c_2 and α_2 are positive scalars. Its time derivative can be written as

$$\dot{V}\left(\tilde{\mathbf{m}}(t), \tilde{\mathbf{v}}(t)\right) = -\alpha_1\|\mathbf{m}(t)\times\hat{\mathbf{m}}(t)\|^2 - c_2\frac{\alpha_0}{\alpha_2}\left[\mathbf{m}(t)\cdot\tilde{\mathbf{v}}(t)\right]^2.$$

As $\dot{V}\left(\tilde{\mathbf{m}}(t), \tilde{\mathbf{v}}(t)\right) \leq 0$ and $V\left(\tilde{\mathbf{m}}(t), \tilde{\mathbf{v}}(t)\right) \geq 0$, it follows that $V\left(\tilde{\mathbf{m}}(t), \tilde{\mathbf{v}}(t)\right)$ is bounded. Using the Rayleigh quotient or by direct inspection, one can write $\frac{1}{2}\min\left(1, c_2/\alpha_2\right)\left\|\begin{bmatrix}\tilde{\mathbf{m}}(t) \\ \tilde{\mathbf{v}}\end{bmatrix}\right\|^2 \leq V\left(\tilde{\mathbf{m}}(t), \tilde{\mathbf{v}}(t)\right)$. Hence, as it has been shown that $V\left(\tilde{\mathbf{m}}(t), \tilde{\mathbf{v}}(t)\right)$ is bounded, the first statement of the theorem is implied, i.e., the error variables $\tilde{\mathbf{m}}(t)$ and $\tilde{\mathbf{v}}(t)$ are bounded. Next, compute the time derivative of $\dot{V}\left(\tilde{\mathbf{m}}(t), \tilde{\mathbf{v}}(t)\right)$, which is given by

$$\begin{aligned} \ddot{V}\left(\tilde{\mathbf{m}}(t), \tilde{\mathbf{v}}(t)\right) = & -2\alpha_1\left[\mathbf{m}(t)\times\hat{\mathbf{m}}(t)\right]\cdot\frac{d}{dt}\left[\mathbf{m}(t)\times\hat{\mathbf{m}}(t)\right] \\ & -2c_2\frac{\alpha_0}{\alpha_2}\left[\mathbf{m}(t)\cdot\tilde{\mathbf{v}}(t)\right]\frac{d}{dt}\left[\mathbf{m}(t)\cdot\tilde{\mathbf{v}}(t)\right], \end{aligned}$$

where $\frac{d}{dt}\left[\mathbf{m}(t)\cdot\tilde{\mathbf{v}}(t)\right] = \dot{\mathbf{m}}(t)\cdot\tilde{\mathbf{v}}(t) + \mathbf{m}(t)\cdot\dot{\tilde{\mathbf{v}}}(t)$ and

$$\begin{aligned} \tfrac{d}{dt}\left[\mathbf{m}(t)\times\hat{\mathbf{m}}(t)\right] = & -\left[\boldsymbol{\omega}_m(t) + c_2\mathbf{v}(t)\right]\times\left[\mathbf{m}(t)\times\hat{\mathbf{m}}(t)\right] \\ & -\alpha_1\left[\mathbf{m}(t)\cdot\hat{\mathbf{m}}(t)\right]\left[\mathbf{m}(t)\times\hat{\mathbf{m}}(t)\right] \\ & +c_2\left[\mathbf{m}(t)\cdot\hat{\mathbf{m}}(t)\right]\tilde{\mathbf{v}}(t) - c_2\left[\mathbf{m}(t)\cdot\tilde{\mathbf{v}}(t)\right]\hat{\mathbf{m}}(t). \end{aligned} \tag{11}$$

Notice that, by definition, $\mathbf{m}(t)$ has constant norm. As $\tilde{\mathbf{m}}(t)$ is bounded, it follows that so are the estimates $\hat{\mathbf{m}}(t)$. In addition, $\mathbf{v}(t)$ also has constant norm and, by assumption, $\boldsymbol{\omega}_m(t)$ is bounded. Also, it has already been shown that $\tilde{\mathbf{v}}(t)$ is bounded. Therefore, one can conclude that all terms in (11) are bounded. On the other hand, as both $\mathbf{m}(t)$ and $\mathbf{v}(t)$ have constant norm and, by assumption, $\boldsymbol{\omega}_m(t)$ is bounded, it follows that $\dot{\mathbf{m}}(t)$

is also bounded. Following similar arguments as before, one can notice that all terms in (10) are bounded and hence $\dot{\tilde{\mathbf{v}}}(t)$ is bounded. Consequently, $\ddot{V}(\tilde{\mathbf{m}}(t), \tilde{\mathbf{v}}(t))$ is also bounded. Thus, one further concludes that $\dot{V}(\tilde{\mathbf{m}}(t), \tilde{\mathbf{v}}(t))$ is uniformly continuous. Moreover, as $\dot{V}(\tilde{\mathbf{m}}(t), \tilde{\mathbf{v}}(t)) \leq 0$ and $V(\tilde{\mathbf{m}}(t), \tilde{\mathbf{v}}(t)) \geq 0$, it follows that $V(\tilde{\mathbf{m}}(t), \tilde{\mathbf{v}}(t))$ converges to a limit. Now, using Barbalat's lemma, one concludes that $\dot{V}(\tilde{\mathbf{m}}(t), \tilde{\mathbf{v}}(t))$ converges to zero, which establishes not only the second statement of the theorem but also that

$$\lim_{t\to\infty} \mathbf{m}(t) \cdot \tilde{\mathbf{v}}(t) = 0. \tag{12}$$

Next, notice that the time derivative of (11) is, under the assumptions of the theorem, bounded, which means that (11) is uniformly continuous. Moreover, from the second statement of the theorem, $\mathbf{m}(t) \times \hat{\mathbf{m}}(t)$ converges to a limit. Therefore, invoking the Barbalat's lemma again, one can conclude that

$$\lim_{t\to\infty} \frac{d}{dt}\left[\mathbf{m}(t) \times \hat{\mathbf{m}}(t)\right] = \mathbf{0}. \tag{13}$$

Now, taking the limit of both sides of (11) and noticing that all quantities therein are bounded, and using (13) as well as the second statement of the theorem, allows one to conclude that

$$\lim_{t\to\infty} \left(\left[\mathbf{m}(t) \cdot \hat{\mathbf{m}}(t)\right] \tilde{\mathbf{v}}(t) - \left[\mathbf{m}(t) \cdot \tilde{\mathbf{v}}(t)\right] \hat{\mathbf{m}}(t)\right) = \mathbf{0}. \tag{14}$$

Using (12) in (14) readily gives

$$\lim_{t\to\infty} \left[\mathbf{m}(t) \cdot \hat{\mathbf{m}}(t)\right] \tilde{\mathbf{v}}(t) = \mathbf{0}. \tag{15}$$

To establish the final result of the theorem, is is important to notice that the observer (9) preserves the norm of the estimates $\hat{\mathbf{m}}(t)$, which can be verified by computing its time derivative, which gives $\frac{d}{dt}\|\hat{\mathbf{m}}(t)\| = 0$. As such, and as by assumption $\|\hat{\mathbf{m}}(t_0)\| = \left\|{}^I\mathbf{m}\right\|$, it follows that $\|\mathbf{m}(t)\| = \|\hat{\mathbf{m}}(t)\|$. Therefore, from the second statement of the theorem, one can conclude that, in the limit, either i) $\hat{\mathbf{m}}(t) = \mathbf{m}(t)$ or ii) $\hat{\mathbf{m}}(t) = -\mathbf{m}(t)$. Either way, one can conclude, from (15), that

$$\lim_{t\to\infty} \pm \left\|{}^I\mathbf{m}\right\|^2 \tilde{\mathbf{v}}(t) = \mathbf{0},$$

which gives the third statement of the theorem. □

The significance of this result is as follows: endowed with estimates $\hat{\mathbf{v}}(t)$ of $\mathbf{v}(t)$, in addition to measurements of $\mathbf{m}(t)$, an estimate of $\boldsymbol{\omega}_E(t)$ is readily given by $\hat{\boldsymbol{\omega}}_E(t) = c_1\mathbf{m}(t) - c_2\hat{\mathbf{v}}(t)$, whose error converges to zero in the conditions of Theorem 1. This allows to drive the nominal attitude dynamics. Moreover, $\mathbf{v}(t)$ corresponds to a known constant inertial vector, as given by (6). An additional similar relation exists for another nonparallel vector, as given by (3). Thus, one has all the necessary ingredients to design an error feedback term to drive the attitude error dynamics to zero, as it will be shown in the next section.

Remark 1. *Notice that, in comparison with the observer proposed in [20], an additional feedback term is now introduced, which allows to obtain a much stronger result. Indeed, in [20] it was shown that*

$$\lim_{t\to\infty} \frac{\mathbf{m}(t)}{\left\|{}^I\mathbf{m}\right\|} \times \left(\tilde{\mathbf{v}}(t) \times \frac{\mathbf{m}(t)}{\left\|{}^I\mathbf{m}\right\|}\right) = \mathbf{0}$$

which means that the projection of the error $\tilde{\mathbf{v}}(t)$ on the plane orthogonal to $\mathbf{m}(t)$ converges to zero. But nothing had been shown about the component of the error $\tilde{\mathbf{v}}(t)$ along the direction of $\mathbf{m}(t)$, so in principle it would be possible for $\tilde{\mathbf{v}}(t) \cdot \mathbf{m}(t)$ to diverge over time. While this would not pose a problem from a theoretical point of view as the estimate $\hat{\mathbf{v}}(t)$ was projected on the plane orthogonal to $\mathbf{m}(t)$ in the second observer, it could pose significant problems to the implementation. The observer that is now proposed completely eliminates this potential pitfall by taking advantage of the fact that, by definition, $\mathbf{v}(t)$ is orthogonal to $\mathbf{m}(t)$. Indeed, the extra feedback term $-\alpha_0\mathbf{m}(t) \cdot \hat{\mathbf{v}}(t)\mathbf{m}(t)$ ensures that, over time, the estimate $\hat{\mathbf{v}}(t)$ has no components along the direction of $\mathbf{m}(t)$. Additionally, this results significantly allows to simplify the structure of the second observer, in comparison with the observer proposed in [20].

3.2. Attitude observer

This section presents the design and stability analysis of an attitude observer based upon the rate gyro measurements $\boldsymbol{\omega}_m(t)$, the estimates of $\mathbf{v}(t)$ provided by the observer (9), and the body-fixed vector measurements $\mathbf{m}(t)$, in addition to the information of the corresponding vectors in inertial coordinates, ${}^I\mathbf{v}$ and ${}^I\mathbf{m}$.

First, substitute (2) in (1), which gives $\dot{\mathbf{R}}(t) = \mathbf{R}(t)\mathbf{S}\left[\boldsymbol{\omega}_m(t) - \boldsymbol{\omega}_E(t)\right]$. Further using the decomposition of the Earth angular velocity (5), one can write the nominal rotation dynamics as

$$\dot{\mathbf{R}}(t) = \mathbf{R}(t)\mathbf{S}\left[\boldsymbol{\omega}_m(t) - c_1\mathbf{m}(t) + c_2\mathbf{v}(t)\right].$$

Consider the attitude observer given by

$$\dot{\hat{\mathbf{R}}}(t) = \hat{\mathbf{R}}(t)\mathbf{S}\left[\boldsymbol{\omega}_o(t)\right], \tag{16}$$

where $\hat{\mathbf{R}}(t) \in SO(3)$ is the attitude estimate, with

$$\begin{aligned} \boldsymbol{\omega}_o(t) \quad := \quad & \boldsymbol{\omega}_m(t) - c_1\mathbf{m}(t) + c_2\hat{\mathbf{v}}(t) \\ & +\alpha_3\mathbf{m}(t) \times \left[\hat{\mathbf{R}}^T(t){}^I\mathbf{m}\right] + \alpha_4\hat{\mathbf{v}}(t) \times \left[\hat{\mathbf{R}}^T(t){}^I\mathbf{v}\right], \end{aligned}$$

where $\alpha_3 \in \mathbb{R}^+$ and $\alpha_4 \in \mathbb{R}^+$ are positive scalar observer gains and $\hat{\mathbf{v}}(t)$ is the estimate provided by (9). The structure of the observer is such that the topological characteristics of $\hat{\mathbf{R}}(t)$ are preserved, i.e., if $\hat{\mathbf{R}}(t_0) \in SO(3)$, then $\hat{\mathbf{R}}(t) \in SO(3)$ for all $t \geq t_0$. Define the error variable $\tilde{\mathbf{R}}(t) = \mathbf{R}(t)\hat{\mathbf{R}}^T(t)$. Notice that, by construction, $\tilde{\mathbf{R}}(t) \in SO(3)$ and the estimation error converges to zero if an only if $\tilde{\mathbf{R}}(t)$ converges to an identity matrix. The error dynamics are given by

$$\dot{\tilde{\mathbf{R}}}(t) = -\mathbf{S}\left[\boldsymbol{\omega}_f(t) + \tilde{\boldsymbol{\omega}}_f(t)\right]\tilde{\mathbf{R}}(t), \tag{17}$$

with $\boldsymbol{\omega}_f(t) := \alpha_3{}^I\mathbf{m} \times \left[\tilde{\mathbf{R}}(t){}^I\mathbf{m}\right] + \alpha_4{}^I\mathbf{v} \times \left[\tilde{\mathbf{R}}(t){}^I\mathbf{v}\right]$ and $\tilde{\boldsymbol{\omega}}_f(t) := -c_2\mathbf{R}(t)\tilde{\mathbf{v}}(t) - \alpha_4\left[\mathbf{R}(t)\tilde{\mathbf{v}}(t)\right] \times \left[\tilde{\mathbf{R}}(t){}^I\mathbf{v}\right]$.

Before proceeding to the main results of the paper, it is convenient to introduce the equivalent error in terms of quaternions [23]. Let $((\tilde{s}(t), \tilde{\mathbf{r}}(t))$ denote the unit quaternion corresponding to the rotation error $\tilde{\mathbf{R}}(t)$, where $\tilde{s}(t)$ and $\tilde{\mathbf{r}}(t)$ are the so-called scalar and vector parts, respectively. The equivalence can be expressed by

$$\tilde{\mathbf{R}}(t) = \mathbf{I} + 2\tilde{s}(t)\mathbf{S}(\tilde{\mathbf{r}}(t)) + 2\left[\mathbf{S}(\tilde{\mathbf{r}}(t))\right]^2$$

and the corresponding quaternion dynamics are given by

$$\begin{cases} \dot{\tilde{s}}(t) = \frac{1}{2}\left[\boldsymbol{\omega}_f(t) + \tilde{\boldsymbol{\omega}}_f(t)\right] \cdot \tilde{\mathbf{r}}(t) \\ \dot{\tilde{\mathbf{r}}}(t) = -\frac{1}{2}\left[\tilde{s}(t)\mathbf{I} - \mathbf{S}(\tilde{\mathbf{r}}(t))\right]\left[\boldsymbol{\omega}_f(t) + \tilde{\boldsymbol{\omega}}_f(t)\right] \end{cases}.$$

Notice that a null estimation error, i.e., $\tilde{\mathbf{R}}(t) = \mathbf{I}$, is equivalent to $\tilde{\mathbf{r}}(t) = \mathbf{0}$.

The following theorem characterizes the input-to-state stability of the attitude error with the error of the auxiliary observer as an input.

Theorem 2. *Define the parameterized set*

$$\mathcal{R}(\epsilon) := \left\{\tilde{\boldsymbol{R}}(\tilde{s}, \tilde{\mathbf{r}}) \in SO(3) : |\tilde{s}| \geq \epsilon\right\}$$

and consider the attitude observer (16)*, where the estimates* $\hat{\mathbf{v}}(t)$ *are obtained using the state observer* (9)*. Further assume that the conditions of Theorem 1 hold and suppose that both* α_3 *and* α_4 *are positive gains. Fix* $0 < \epsilon < 1$*,* $0 < \theta < 1$*, and define*

$$\beta_1 := \frac{\alpha_3\alpha_4}{\alpha_3\left\|{}^I\mathbf{m}\right\|^2 + \alpha_4\left\|{}^I\mathbf{v}\right\|^2}\left\|{}^I\mathbf{m} \times {}^I\mathbf{v}\right\|^2,$$

$$\beta_2 := c_2 + \alpha_4\left\|{}^I\mathbf{v}\right\|,\ \beta_3 := \frac{\beta_2}{2\theta\beta_1\epsilon^2},\ r_v := \frac{\sqrt{1-\epsilon^2}}{\beta_3}.$$

Then, the dynamics of $\tilde{\mathbf{r}}(t)$ *are locally input-to-state stable with respect to* $\tilde{\mathbf{v}}(t)$*, with* $\tilde{\boldsymbol{R}}(t_0) \in \mathcal{R}(\epsilon)$ *and* $\sup_{t\geq t_0}\|\tilde{\mathbf{v}}(t)\| < r_v$.

Proof. Define the Lyapunov-like function $V(\tilde{\mathbf{r}}(t)) := \frac{1}{2}\|\tilde{\mathbf{r}}(t)\|^2$ and take its time derivative, which can written as

$$\dot{V}(\tilde{\mathbf{r}}(t)) = -\frac{1}{2}\tilde{s}(t)\boldsymbol{\omega}_f(t) \cdot \tilde{\mathbf{r}}(t) - \frac{1}{2}\tilde{s}(t)\tilde{\boldsymbol{\omega}}_f(t) \cdot \tilde{\mathbf{r}}(t). \tag{18}$$

Computing the first term of (18) gives, after some long but tedious computations,

$$\begin{aligned} -\tfrac{1}{2}\tilde{s}(t)\boldsymbol{\omega}_f(t) \cdot \tilde{\mathbf{r}}(t) = &-\alpha_3\tilde{s}^2(t)\left\|\tilde{\mathbf{r}}(t) \times {}^I\mathbf{m}\right\|^2 \\ &-\alpha_4\tilde{s}^2(t)\left\|\tilde{\mathbf{r}}(t) \times {}^I\mathbf{v}\right\|^2. \end{aligned} \tag{19}$$

Consider now the property that states that, given two unit vectors $\mathbf{x}, \mathbf{y} \in \mathbb{R}^3$ and two positive scalars k_x and k_y then, for all vectors $\mathbf{z} \in \mathbb{R}^3$, it is true that

$$k_x\|\mathbf{z} \times \mathbf{x}\|^2 + k_y\|\mathbf{z} \times \mathbf{y}\|^2 \geq \frac{k_x k_y}{k_x + k_y}\|\mathbf{z}\|^2\|\mathbf{x} \times \mathbf{y}\|^2,$$

see [5]. Applying it to (19) readily gives

$$-\tfrac{1}{2}\tilde{s}(t)\boldsymbol{\omega}_f(t) \cdot \tilde{\mathbf{r}}(t) \leq -\beta_1\tilde{s}^2(t)\|\tilde{\mathbf{r}}(t)\|^2. \tag{20}$$

Notice that, under Assumption 1 and the conditions of the theorem, β_1 is a positive constant. On the other hand, using simple inequalities, it is possible to bound the second term of (18) by

$$-\frac{1}{2}\tilde{s}(t)\tilde{\boldsymbol{\omega}}_f(t) \cdot \tilde{\mathbf{r}}(t) \leq \frac{1}{2}|\tilde{s}(t)|\|\tilde{\mathbf{r}}(t)\|\left\|\tilde{\boldsymbol{\omega}}_f(t)\right\|.$$

Using simple norm inequalities, one can show that $\left\|\tilde{\boldsymbol{\omega}}_f(t)\right\| \leq \beta_2\|\tilde{\mathbf{v}}(t)\|$. Notice that, in the conditions of the Theorem, β_2 is a positive constant. Additionally, by definition, $|\tilde{s}(t)| \leq 1$. Therefore,

$$-\frac{1}{2}\tilde{s}(t)\tilde{\boldsymbol{\omega}}_f(t) \cdot \tilde{\mathbf{r}}(t) \leq \frac{\beta_2}{2}\|\tilde{\mathbf{r}}(t)\|\|\tilde{\mathbf{v}}(t)\|. \tag{21}$$

Using the bounds (20) and (21) in (18) allows one to write

$$\dot{V}(\tilde{\mathbf{r}}(t)) \leq -\|\tilde{\mathbf{r}}(t)\|\left(\beta_1\tilde{s}^2(t)\|\tilde{\mathbf{r}}(t)\| - \frac{\beta_2}{2}\|\tilde{\mathbf{v}}(t)\|\right). \tag{22}$$

Now, fix $0 < \theta < 1$. Then, using also the fact that $\tilde{s}^2(t) = 1 - \|\tilde{\mathbf{r}}(t)\|^2$, one can write, from (22), that

$$\begin{aligned} \dot{V}(\tilde{\mathbf{r}}(t)) \leq &-(1-\theta)\beta_1\|\tilde{\mathbf{r}}(t)\|^2\left(1 - \|\tilde{\mathbf{r}}(t)\|^2\right) \\ &-\|\tilde{\mathbf{r}}(t)\|\left(\theta\beta_1\left(\|\tilde{\mathbf{r}}(t)\| - \|\tilde{\mathbf{r}}(t)\|^3\right) - \beta_2/2\|\tilde{\mathbf{v}}(t)\|\right). \end{aligned}$$

Then, it is a simple matter of computation to conclude that

$$\begin{aligned} \dot{V}(\tilde{\mathbf{r}}(t)) \quad \leq \quad &-(1-\theta)\beta_1\epsilon^2\|\tilde{\mathbf{r}}(t)\|^2 \\ &-\|\tilde{\mathbf{r}}(t)\|\left(\theta\beta_1\epsilon^2\|\tilde{\mathbf{r}}(t)\| - \beta_2/2\|\tilde{\mathbf{v}}(t)\|\right) \end{aligned}$$

for all $\|\tilde{\mathbf{r}}(t)\| \leq \sqrt{1-\epsilon^2}$ and hence

$$\dot{V}(\tilde{\mathbf{r}}(t)) \leq -(1-\theta)\beta_1\epsilon^2\|\tilde{\mathbf{r}}(t)\|^2$$

for all

$$\beta_3\|\tilde{\mathbf{v}}(t)\| \leq \|\tilde{\mathbf{r}}(t)\| \leq \sqrt{1-\epsilon^2}.$$

The proof is concluded invoking [19, Theorem 5.2]. □

Notice that, in the definition of the region of convergence $\mathcal{R}(\epsilon)$ in Theorem 2, ϵ can be chosen as an arbitrarily small positive constant, which is equivalent to say that the initial error rotation angle must be smaller than π by an arbitrarily small positive margin. Therefore, the result is better characterized as semi-global in what concerns the initial attitude error, in the same way as in [3, Theorem 2]. There is also a restriction on the input error $\tilde{\mathbf{v}}(t)$. However, it is important to recall that this error converges to zero, so there exists a certain time instant after which $\tilde{\mathbf{v}}(t)$ is small enough so that Theorem 2 applies.

The next result establishes a local stability result considering the overall cascaded system and gives insight to the local behavior of the system.

Theorem 3. *Consider the observer given by* (9) *and* (16) *under Assumption 1 and 2. Further suppose that* $\alpha_i > 0$*,* $i = 0, \ldots, 4$*. Then, the origin of* $\left(\mathbf{m}(t) \times \hat{\mathbf{m}}(t), \tilde{\mathbf{v}}(t), \tilde{\boldsymbol{R}}(t) - \mathbf{I}\right)$ *corresponding to* $\mathbf{m}(t) = \hat{\mathbf{m}}(t)$*,* $\tilde{\mathbf{v}}(t) = \mathbf{0}$*, and* $\tilde{\boldsymbol{R}}(t) = \mathbf{I}$ *is a local exponentially stable equilibrium point.*

Proof. The proof follows by showing that the linearized dynamics of $\left(\mathbf{m}(t)\times\hat{\mathbf{m}}(t), \tilde{\mathbf{v}}(t), \tilde{\mathbf{R}}(t)-\mathbf{I}\right)$ around $\mathbf{m}(t) = \hat{\mathbf{m}}(t)$, $\tilde{\mathbf{v}}(t) = \mathbf{0}$, and $\tilde{\mathbf{R}}(t) = \mathbf{I}$ are exponentially stable. It is a matter of computation to show that the linearized dynamics of $\mathbf{m}(t)\times\hat{\mathbf{m}}(t)$ and $\tilde{\mathbf{v}}(t)$ are given by

$$\begin{aligned}\dot{\mathbf{x}}_1(t) &= -\alpha_1\left\|{}^I\mathbf{m}\right\|^2\mathbf{x}_1 - \mathbf{S}\left[\omega_m(t) + c_2\mathbf{v}(t)\right]\mathbf{x}_1(t)\\ &\quad + c_2\left\|{}^I\mathbf{m}\right\|^2\mathbf{x}_2 - c_2\mathbf{m}(t)\cdot\mathbf{x}_2(t)\mathbf{m}(t)\end{aligned}$$

and

$$\begin{aligned}\dot{\mathbf{x}}_2(t) &= -\alpha_2\mathbf{x}_1(t) - \alpha_0\mathbf{m}(t)\cdot\mathbf{x}_2(t)\mathbf{m}(t)\\ &\quad -\mathbf{S}\left[\omega_m(t) - c_1\mathbf{m}(t)\right]\mathbf{x}_2(t),\end{aligned}$$

respectively, where $\mathbf{x}_1(t)\in\mathbb{R}^3$ and $\mathbf{x}_2(t)\in\mathbb{R}^3$ were introduced as incremental variables for the linearization of the nonlinear dynamics of $\mathbf{m}(t)\times\hat{\mathbf{m}}(t)$ and $\tilde{\mathbf{v}}(t)$, respectively. Consider now the linearization of the attitude error dynamics given by $\tilde{\mathbf{R}}(t)\approx\mathbf{I}+\mathbf{S}\left[\mathbf{x}_3(t)\right]$, $\mathbf{x}_3(t)\in\mathbb{R}^3$, see e.g. [8]. Notice that, for the linearization of $\tilde{\mathbf{R}}(t)-\mathbf{I}$ around the origin, one has $\mathbf{x}_3(t) = \mathbf{0}$, and the linearized error dynamics are given by

$$\begin{aligned}\dot{\mathbf{x}}_3(t) &= \left[\alpha_3\mathbf{S}^2\left({}^I\mathbf{m}\right) + \alpha_4\mathbf{S}^2\left({}^I\mathbf{v}\right)\right]\mathbf{x}_3(t)\\ &\quad + c_2\mathbf{R}(t)\mathbf{x}_2(t) - \alpha_4\mathbf{S}\left({}^I\mathbf{v}\right)\mathbf{R}(t)\mathbf{x}_2(t).\end{aligned}$$

To show that the linearized error dynamics are stable, consider the Lyapunov transformation given by

$$\mathbf{z}(t) = \begin{bmatrix}\mathbf{R}(t)\mathbf{x}_1(t)\\ \mathbf{R}(t)\mathbf{x}_2(t)\\ \mathbf{x}_3(t)\end{bmatrix},$$

which preserves stability and convergence properties. Then, one can show that $\dot{\mathbf{z}}(t) = \mathbf{A}\mathbf{z}(t)$, where

$$\mathbf{A} = \begin{bmatrix}\mathbf{A}_1 & \mathbf{0}\\ \mathbf{A}_{21} & \alpha_3\mathbf{S}^2\left({}^I\mathbf{m}\right) + \alpha_4\mathbf{S}^2\left({}^I\mathbf{v}\right)\end{bmatrix}$$

is a stable Hurwitz matrix in the conditions of the theorem, with $\mathbf{A}_{21} = c_2\mathbf{I} - \alpha_4\mathbf{S}\left({}^I\mathbf{v}\right)$ and

$$\mathbf{A}_1 = \begin{bmatrix}-\alpha_1\left\|{}^I\mathbf{m}\right\|^2\mathbf{I} - c_1\mathbf{S}\left({}^I\mathbf{m}\right) & c_2\left\|{}^I\mathbf{m}\right\|^2\mathbf{I} - c_2^I\mathbf{m}^I\mathbf{m}^T\\ -\alpha_2\mathbf{I} & -\alpha_0^I\mathbf{m}^I\mathbf{m}^T + c_2\mathbf{S}\left({}^I\mathbf{v}\right)\end{bmatrix},$$

thus concluding the proof. □

Finally, in this paper only one body-fixed vector measurement was considered, as it is the most demanding (and interesting) case from the theoretical point of view. Nevertheless, the structure of the observer can be extended to include additional body-fixed vector measurements.

4. Simulation results

Simulation results are presented in this section to demonstrate the performance achieved with the proposed solution. The local inertial frame was considered as the NED frame, centered at a latitude of $\varphi = 38.7138°$, a longitude of $\psi = 9.1394°$, and at sea level. The norm of the angular velocity of the Earth was set to $\left\|{}^I\omega_E\right\| = 7.2921150\times10^{-5}$ rad/s, which corresponds approximately to 15 degrees per hour. Thus, in the NED frame, one has ${}^I\omega_E = \left\|{}^I\omega_E\right\|\begin{bmatrix}\cos\varphi & 0 & -\sin\varphi\end{bmatrix}^T$. As for the vector measurement $\mathbf{m}(t)$, it is assumed that magnetic field measurements are available. However, any other inertial vector could have been considered. In this case, the 11th generation of International Geomagnetic Reference Field was employed for the latitude, longitude, and altitude previously described, which gives ${}^I\mathbf{m}\approx[2.6338\ 0.0851\ 3.6359]^T\times10^4$ (nT). Notice that, with this choice, Assumption 1 is satisfied.

Table 1: Observer gains for (9)

Time (s)	$\alpha_1\left\|{}^I\mathbf{m}\right\|^2$	α_2
$[0, 300[$	10	10×10^{-2}
$[300, 420[$	10	5×10^{-2}
$[420, 600[$	5	2.5×10^{-2}
$[600, 720[$	2.5	1×10^{-2}
$[720, +\infty[$	2.5	5×10^{-3}

The initial attitude of the platform was set to $\mathbf{R}(0) = \mathbf{I}$ and the evolution of the angular velocity is given by

$$\omega(t) = \begin{bmatrix}5\frac{\pi}{180}\sin\left(\frac{2\pi}{60}t\right)\\ \frac{\pi}{180}\sin\left(\frac{2\pi}{180}t\right)\\ -2\frac{\pi}{180}\sin\left(\frac{2\pi}{300}t\right)\end{bmatrix}(\mathrm{rad/s}).$$

In order to demonstrate the robustness of the proposed solutions to sensor measurement errors, the measurements of the magnetometer were assumed to be corrupted by zero-mean white Gaussian noise, with standard deviation of 150 nT, which corresponds to the worst case specification of the triaxial magnetometer of the nanoIMU NA02-0150F50. The rate gyro measurements are also to be corrupted by noise, characterized by an angle random walk of $4°/\mathrm{hr}/\sqrt{\mathrm{Hz}}$, which corresponds to the KVH DSP-3000 fiber optic gyro. A sampling frequency of 100 Hz was considered and the fourth-order Runge-Kutta method was employed in the simulations.

In order to ensure both fast convergence speed and good steady-state performance of the observer, a set of piece-wise constant gains was chosen for the first block. In terms of the actual convergence results, it is important to stress that the use of these gains does not have any significant impact. This is so because the number of transitions is finite, i.e., the gains remain constant for all $t\geq t_s$, where t_s corresponds to the last transition time instant. Hence, all the stability and convergence results derived in the paper apply considering t_s as the initial time instant. These gains are described in Table 1, whereas $\alpha_0 = 0.1/\left\|{}^I\mathbf{m}\right\|^2$. As for the second block, the gains were set to $\alpha_3 = \frac{0.02}{\|{}^I\mathbf{m}\|^2}$ and $\alpha_4 = \frac{0.4}{\|{}^I\mathbf{v}\|^2}$. As in most nonlinear observers, these gains were chosen empirically, although the relative gains of the second observer are related to the error noise of its observations. The initial estimate of the first observer $\hat{\mathbf{m}}(0)$ was set identical to the first measurement, while $\hat{\mathbf{v}}(0)$ was set to zero. The initial attitude estimate was set such that the initial rotation angle error is very close to 180 degrees.

The initial convergence of the errors $\tilde{\mathbf{m}}(t)$ and $\tilde{\mathbf{v}}(t)$ is depicted in Fig. 2. While the convergence of the observer is fast, different gains are required, as detailed in Table 1, in order to ensure an adequate steady-state level of performance, as it will be detailed shortly. The initial convergence of the attitude error $\tilde{\mathbf{R}}(t) - \mathbf{I}$ is shown in Fig. 3. These plots show that the error converges to a neighborhood of zero. In the absence of noise, the errors converge to zero.

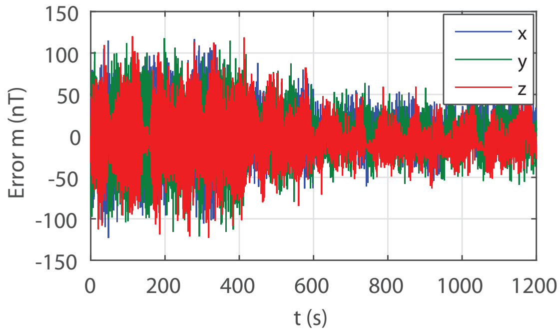

(a) Error $\tilde{\mathbf{m}}(t)$

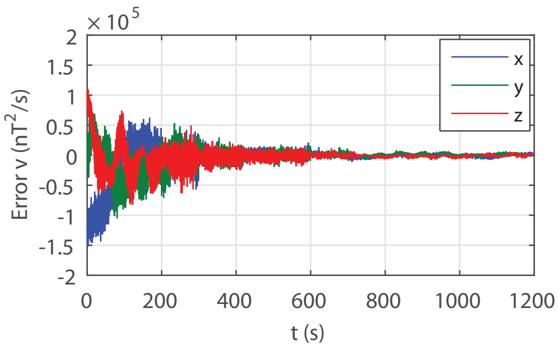

(b) Error $\frac{\mathbf{m}(t)}{\|^I\mathbf{m}\|} \times \left(\tilde{\mathbf{v}}(t) \times \frac{\mathbf{m}(t)}{\|^I\mathbf{m}\|}\right)$

Figure 2: Initial convergence of the errors of (10)

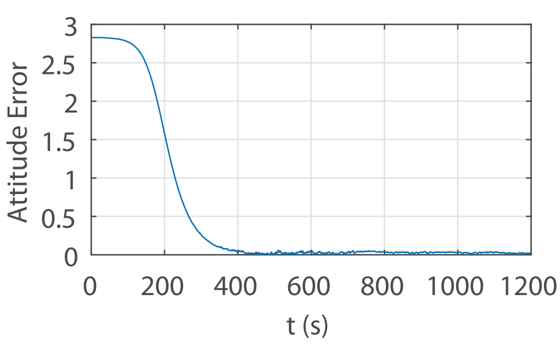

Figure 3: Initial convergence of the error $\left\|\tilde{\mathbf{R}}(t) - \mathbf{I}\right\|$

In order to evaluate the performance of the attitude observer, the steady-state standard deviation of the errors is depicted in Table 2. These values should be compared to the magnitude of the corresponding variables, which is roughly 4.5×10^4 nT for $\mathbf{m}(t)$ and 1.5×10^5 nT^2/s for $\mathbf{v}(t)$. Evidently, the observer achieves very good results. Using the Euler angle-axis representation for the rotation error,

Table 2: Standard deviation of the steady-state error of the observer on $SO(3)$ - the mean value of the standard deviation for each element of the errors is shown

Variable	Standard deviation
$\tilde{\mathbf{m}}(t)$ (nT)	16.6
$\tilde{\mathbf{v}}(t)$ (nT^2/s)	1738
$\tilde{\mathbf{R}}(t) - \mathbf{I}$	0.004

$$\begin{aligned}\tilde{\mathbf{R}}(t) &= \mathbf{I}\cos\left(\tilde{\theta}(t)\right) + \left[1 - \cos\left(\tilde{\theta}(t)\right)\right]\tilde{\mathbf{d}}(t)\tilde{\mathbf{d}}^T(t) \\ &\quad -\mathbf{S}\left(\tilde{\mathbf{d}}(t)\right)\sin\left(\tilde{\theta}(t)\right),\end{aligned} \tag{23}$$

where $0 \leq \tilde{\theta}(t) \leq \pi$ and $\tilde{\mathbf{d}}(t) \in \mathbb{R}^3$, $\left\|\tilde{\mathbf{d}}(t)\right\| = 1$, are the angle and axis that represent the rotation error, the performance of the proposed solution is identified from the evolution of $\tilde{\theta}$, which is depicted, after the initial transients fade out, in Fig. 4. The mean angle error, computed for $t \geq 2400$ s, is 0.636°, which is a very good result.

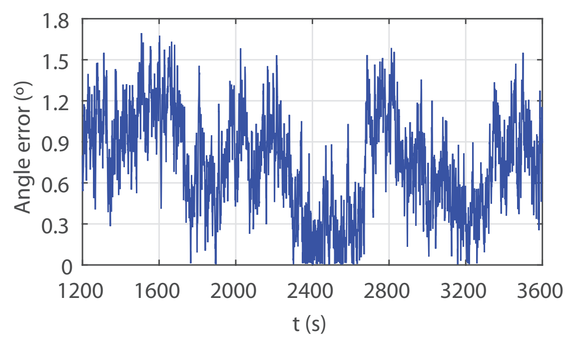

Figure 4: Evolution of the angle error $\tilde{\theta}(t)$

In order to better evaluate the performance of the proposed solution, the Monte Carlo method was applied, and 1000 simulations were carried out with different, randomly generated noise signals. The mean angle error, using the Euler angle-axis representation (23), was computed for each simulation, for $t \geq 2400$ s, and averaged over the set of simulations. The resulting mean angle error was 0.42°.

In the simulations that were presented insofar the angular velocity of the body does not exceed $5°/s$ around each principal axis. Hence, it is only natural to ask if much higher angular velocities have any impact whatsoever in the convergence speed or steady-state performance of the proposed solution. As it turns out, the proposed solutions can effectively handle much higher velocities. To exemplify that situation, the previous simulation was modified considering an angular velocity 20 times higher than the previous one, as given by

$$\boldsymbol{\omega}(t) = \begin{bmatrix} 100\frac{\pi}{180}\sin\left(\frac{2\pi}{60}t\right) \\ 20\frac{\pi}{180}\sin\left(\frac{2\pi}{180}t\right) \\ -40\frac{\pi}{180}\sin\left(\frac{2\pi}{300}t\right) \end{bmatrix} (\mathrm{rad}/s)\,.$$

As it turns out, there are no notable differences in terms of initial convergence, which is very similar to that of Figures 2 and 3. This is not surprising as, in the error dynamics (10), the angular velocity appears through skew-symmetric terms, hence the norm of the error would not be affected if those were the only terms in the error dynamics. On the other hand, the angular velocity does not appear in the error dynamics (17). To evaluate the steady-state performance, the Monte Carlo method was applied, and 1000 simulations were carried out with different, randomly generated noise signals. The mean angle error, using the Euler angle-axis representation (23), was computed for each simulation, for $t \geq 2400$ s, and averaged over the set of simulations. The resulting mean angle error was 0.51°, which corresponds only to a slight decrease in performance.

5. Conclusions

This paper proposed a new attitude observer that is based solely on measurements of a single body-fixed vector and the angular velocity provided by a set of three high-grade rate gyros, sensitive to the angular velocity of the Earth about its own axis. This is in contrast with typical solutions that require two observations of inertial vectors. The key idea of the observer, which is cascaded, is to first obtain an estimate of a second vector in body-fixed coordinates that corresponds to a constant known vector in inertial coordinates, and that also allows one to estimate the angular velocity of the Earth. Then, a second block is proposed, directly on the special orthogonal group $SO(3)$, and the estimation error is shown to converge to zero with a large region of attraction (best characterized by an initial error corresponding to a rotation by an angle smaller than 180 degrees by an arbitrarily small positive margin). Locally, the error was shown to be exponentially stable. Simulations are presented, including Monte Carlo results, that illustrate the achievable performance of the proposed observer. Future work includes the estimation/compensation of rate gyro bias.

Acknowledgment

This work was supported by the Fundação para a Ciência e a Tecnologia (FCT) through ISR under FCT [UID/EEA/50009/2013] and through the FCT project DECENTER [LISBOA-01-0145-FEDER-029605], funded by the Lisboa 2020 and PIDDAC programs, and through IDMEC, under LAETA UID/EMS/50022/2013 contracts, by the Macao Science and Technology Development Fund under Grant FDCT/026/2017/A1, and by the University of Macau, Macao, China, under Project MYRG2018-00198-FST.

References

[1] G. Wahba, A Least Squares Estimate of Spacecraft Attitude, SIAM Review 7 (3) (1965) 409.

[2] J. Crassidis, F. Markley, Y. Cheng, Survey of Nonlinear Attitude Estimation Methods, Journal of Guidance, Control and Dynamics 30 (1) (2007) 12–28.

[3] H. Grip, T. Fossen, T. Johansen, A. Saberi, Attitude Estimation Using Biased Gyro and Vector Measurements with Time-Varying Reference Vectors, IEEE Transactions on Automatic Control 57 (5) (2012) 1332–1338.

[4] A. Barrau, S. Bonnabel, The invariant extended Kalman filter as a stable observer, IEEE Transactions on Automatic Control 62 (4) (2017) 1797–1812.

[5] M.-D. Hua, Attitude estimation for accelerated vehicles using GPS/INS measurements, Control Engineering Practice 18 (7) (2010) 723–732.

[6] H. Rehbinder, B. Ghosh, Pose Estimation Using Line-Based Dynamic Vision and Inertial Sensors, IEEE Transactions on Automatic Control 48 (2) (2003) 186–199.

[7] A. Roberts, A. Tayebi, On the Attitude Estimation of Accelerating Rigid-Bodies Using GPS and IMU Measurements, in: Proceedings of the 50th IEEE Conference on Decision and Control, Orlando, USA, 2011, pp. 8088–8093.

[8] R. Mahony, T. Hamel, J.-M. Pflimlin, Nonlinear Complementary Filters on the Special Orthogonal Group, IEEE Transactions on Automatic Control 53 (5) (2008) 1203–1218.

[9] S. Berkane, A. Abdessameud, A. Tayebi, Global hybrid attitude estimation on the special orthogonal group SO(3), in: Proceedings of the 2016 American Control Conference, Boston, USA, 2016, pp. 113–118.

[10] M. Zamani, J. Trumpf, R. Mahony, Minimum-Energy Filtering for Attitude Estimation, IEEE Transactions on Automatic Control 58 (11) (2013) 2917–2921.

[11] A. Sanyal, T. Lee, M. Leok, N. McClamroch, Global optimal attitude estimation using uncertainty ellipsoids, Systems & Control Letters 57 (2008) 236–245.

[12] P. Batista, C. Silvestre, P. Oliveira, Globally Exponentially Stable Cascade Observers for Attitude Estimation, Control Engineering Practice 20 (2) (2012) 148–155.

[13] P. Batista, C. Silvestre, P. Oliveira, Sensor-based Globally Asymptotically Stable Filters for Attitude Estimation: Analysis, Design, and Performance Evaluation, IEEE Transactions on Automatic Control 57 (8) (2012) 2095–2100.

[14] J. Kinsey, L. Whitcomb, Adaptive Identification on the Group of Rigid Body Rotations and its Application to Precision Underwater Robot Navigation, IEEE Transactions on Robotics 23 (1) (2007) 124–136.

[15] J. Trumpf, R. Mahony, T. Hamel, C. Lageman, Analysis of Non-Linear Attitude Observers for Time-Varying Reference Measurements, IEEE Transactions on Automatic Control 57 (11) (2012) 2789–2800.

[16] A. Khosravian, M. Namvar, Rigid Body Attitude Control Using a Single Vector Measurement and Gyro, IEEE Transactions on Automatic Control 57 (5) (2012) 1273–1279.

[17] P. Batista, C. Silvestre, P. Oliveira, A GES Attitude Observer with Single Vector Observations, Automatica 48 (2) (2012) 388–395.

[18] M. Namvar, F. Safaei, Adaptive Compensation of Gyro Bias in Rigid-Body Attitude Estimation Using a Single Vector Measurement, IEEE Transactions on Automatic Control 58 (7) (2013) 1816–1822.

[19] H. Khalil, Nonlinear Systems, 2nd Edition, Prentice-Hall, 1996.

[20] P. Batista, C. Silvestre, P. Oliveira, Attitude and Earth Velocity Estimation - Part II: Observer on the Special Orthogonal Group, in: Proceedings of the 53rd IEEE Conference on Decision and Control, Los Angeles, USA, 2014, pp. 127–132.

[21] P. Batista, C. Silvestre, P. Oliveira, Attitude and Earth Velocity Estimation - Part I: Globally Exponentially Stable Observer, in: Proceedings of the 53rd IEEE Conference on Decision and Control, Los Angeles, USA, 2014, pp. 121–126.

[22] H. Grip, T. Fossen, T. Johansen, A. Saberi, Observers for interconnected nonlinear and linear systems, Automatica 48 (7) (2012) 1339–1346.

[23] T. Fossen, Handbook of Marine Craft Hydrodynamics and Motion Control, Wiley, 2011.